INVESTIGATIONS ON CYLINDRICAL MICROPHONE ARRAYS

FABIO KAISER[1], HANNES POMBERGER[2], FRANZ ZOTTER[2]

[1]Student,
[2]Institute of Electronic Music and Acoustics,
University of Music and Performing Arts Graz, Austria

This contribution discusses sound field recording with microphone arrays on the finite rigid cylinder. Sound field analysis with rigid cylinders has been discussed most often using the solutions of the Helmholtz equation in two dimensions. Rigid cylindrical arrays of finite length cannot be formulated in such an elegant way. Nevertheless, it is possible to simulate a rigid cylindrical array using the boundary element method to obtain the responses to an incident field. To compare the characteristics of rigid cylinder arrays to rigid spherical arrays, the incident field is expanded into spherical harmonics
. For both spherical and cylindrical arrays, the decomposition with regard to azimuth is easily achieved in terms of trigonometric functions, even when only using microphones on the equatorial plane. Discrimination between different elevation angles is improved by adding more microphones on different heights on the cylinder. This is shown for cylindrical bodies with different diameter-to-height ratios in

INTRODUCTION

Compact microphone arrays are used for sound field analysis (source localization, source identification), spatial sound recording, spatial filtering of sound (beamforming) and can be found in various applications from speech recognition to room acoustical measurements. Especially compact spherical microphone arrays received special attention over the last decade because of the uniform treatment of all directions which is crucial for the capture and reproduction of 3D acoustical scenes, cf. [1, 2, 3]. However, in some given acoustical scenes the sound sources can be constrained only to a certain area, letting spherical arrays seem redundant. For that purpose hemispherical arrays have been investigated, see [4], and also circular arrays mounted on a rigid cylinder, cf. [5, 6].

Fig. 1 shows different rigid shapes for microphone array geometries. The sound pressure distribution is assumed to be available on the horizontal ring in Fig. 1(a), or on a ribbon around the horizon in Fig. 1(b). As this pressure distribution is the basis of array signal processing, it is simulated and used in order to compare the different resolution properties of these array types. Correlations of the pressure distributions due to different plane waves carries information about the spatial resolution. We propose a method to find the resolution limits by investigating the correlation matrices of paired

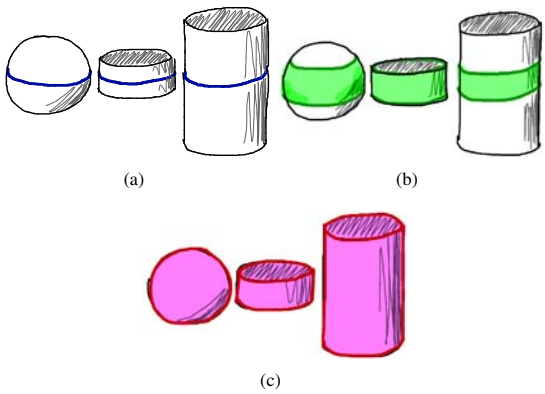

Fig. 1. Different array shapes whose resolution properties are to be estimated: (a) ring arrays on a sphere and cylinders of different lengths, (b) ribbon arrays on a sphere and cylinders of different lengths., and (c) the entire shape used as array

plane waves. The determinant of these correlation matrices measures the discriminability
and is used to indicate difference angles above which two plane waves can be distinguished.

ANALYTIC DESCRIPTION OF RIGID CYLINDRICAL AND SPHERICAL SCATTERERS

In this section the analytical description of a cylindrical and a spherical scatterer is reviewed.

The Helmholtz equation is given by

$$\Delta p(\mathbf{r}) + k^2 p(\mathbf{r}) = 0\,, \qquad (1)$$

where $p(\mathbf{r})$ is the sound pressure at a certain location $\mathbf{r} = [\rho, \phi, z]$, k is the wavenumber, and Δ is the Laplace operator in cylindrical coordinates (Fig. 2).

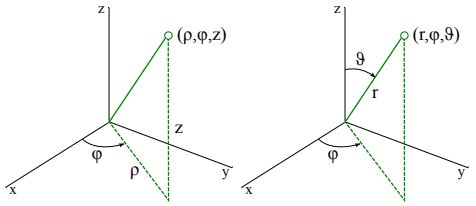

(a) Cylindrical (b) Spherical

Fig. 2. Cylindrical and spherical coordinate system. Cylinder: $\rho = \sqrt{x^2 + y^2}$, $\varphi = \arctan(\frac{y}{x})$ **and** $z = z$. **Sphere:** $r = \sqrt{x^2 + y^2 + z^2}$, $\varphi = \arctan(\frac{y}{x})$ **and** $\vartheta = \arctan\frac{z}{r}$. **The domain of definition is** $\rho, r \in [0, \infty)$, $\varphi \in [0, 2\pi)$, $z \in (-\infty, \infty)$ **and** $\vartheta \in [0, \pi]$.

Cylinder

The scattering of a plane wave incident on a rigid cylinder is most often described by assuming the cylinder to be of infinite length. The one dimensional plane waves scattered on an infinite cylinder only need to satisfy the radiation condition in the cylindrical radius. Hence the following solution is correct, cf. [7, 8, 9], for the sound pressure on the cylinder due to a plane wave from ϕ_0, ϑ_0

$$p(k, z, \phi) = \sum_{m=-\infty}^{\infty} \frac{2\pi \mathrm{i}^{m+1}\, \Phi_m(\phi_0)\Phi_m(\phi)\, e^{\mathrm{i}k\cos\vartheta_0 z}}{k\mathrm{R}\sin\vartheta_0 H_{m'}^{(2)}(k\mathrm{R}\sin\vartheta_0)}, \qquad (2)$$

where R is the radius of the cylinder, $H_n^{\prime(2)}(k\mathrm{R}\sin\vartheta_0)$ is the first derivative of the Hankel function of the second kind, and $\Phi_m(\phi)$ are the normalized trigonometric functions

$$\Phi_m = \sqrt{\frac{2-\delta_m}{2\pi}} \begin{cases} \cos(m\phi), & \text{form} \le 0, \\ \sin(m\phi), & \text{form} < 0. \end{cases} \qquad (3)$$

The term $k\mathrm{R}\sin\vartheta_0 H_{n'}^{(2)}(k\mathrm{R}\sin\vartheta_0)$ will not become zero for $\vartheta_0 = 0$; it is proportional to $\left(\frac{2}{k\mathrm{R}\sin\vartheta_0}\right)^n$ for small arguments.

The solution for a finite-length cylinder cannot be given in closed form [7, p. 31], and fulfilling of the 3D radiation condition becomes necessary. It seems the scattering off a finite-length cylinder has to be simulated numerically using other methods.

Sphere

The scattering response of a plane wave impinging from φ_0, ϑ_0 on a rigid sphere is given by

$$p(k, \phi, \vartheta) = \sum_{n=0}^{\infty} \sum_{m=-n}^{n} \frac{4\pi \mathrm{i}^{n-1}\, Y_n^m(\phi_0, \vartheta_0) Y_n^m(\phi, \vartheta)}{(k\mathrm{R})^2 h_{n'}^{(2)}(k\mathrm{R})}, \qquad (4)$$

where $h_n^{\prime(2)}(kR)$ is the spherical Hankel function of the second kind, and the real valued spherical harmonics $Y_n^m(\phi, \vartheta)$ are defined as

$$Y_n^m(\phi, \vartheta) = \sqrt{\frac{(2n+1)(n-m)!}{2(n+m)!}} P_n^m(\cos\vartheta)\, \Phi_m(\phi)\,, \qquad (5)$$

using the trigonometric functions Eq. (3) and the associated Legendre functions $P_n^m(\cos\vartheta)$ with their normalization factor, cf. [9].

NUMERICAL DESCRIPTION OF CYLINDRICAL SCATTERERS

Analytic solutions for scattering problems with arbitrary geometries are not available. However, such problems can be solved numerically with the Boundary Element Method (BEM), cf. [10] [11]. We use this method to calculate the sound pressure on the surface of a finite-length rigid cylinder for plane waves impinging from different directions.

Helmholtz Integral Equation

The Helmholtz integral equation (HIE) describes the sound pressure in a homogeneous volume V of air by integration of a weighted continuous distribution of point sources (monopoles) and their normal derivative (dipoles) over the volume boundary ∂V,

$$C(\mathbf{r}')p(\mathbf{r}') = \iint_{\partial V} \left(p(r)\frac{\partial G(\mathbf{r}\,|\,\mathbf{r}')}{\partial \mathbf{n}} - \frac{\partial p(\mathbf{r})}{\partial \mathbf{n}} G(\mathbf{r}\,|\,\mathbf{r}')\right) dS + p^I, \qquad (6)$$

where $\mathbf{r}$ lies on the boundary and $\mathbf{r}'$ is the observation point. The terms $p(\mathbf{r})$, and $\frac{\partial p(\mathbf{r})}{\partial \mathbf{n}}$ are the boundary sound pressure and its normal derivative, respectively; $G(\mathbf{r}\,|\,\mathbf{r}') = \frac{e^{-ik\|\mathbf{r}-\mathbf{r}'\|}}{\|\mathbf{r}-\mathbf{r}'\|}$ is the Green's function, and $\frac{\partial G(\mathbf{r}\,|\,\mathbf{r}')}{\partial \mathbf{n}}$ its normal derivative. The term $p^I(\mathbf{r}')$ describes the free field sound pressure on the boundary and is expressed by

$$p^I = e^{\mathrm{i}k(x\cos\phi_0\sin\vartheta_0 + y\sin\phi_0\sin\vartheta_0 + z\sin\vartheta_0)}, \qquad (7)$$

for a plane wave impinging from φ_0, ϑ_0. The weight function $C(\mathbf{r}')$ depends on the location of the

observation point $\mathbf{r}'$ with respect to the volume V of the medium

$$C(\mathbf{r}') = \begin{cases} 0, & \mathbf{r}' \notin V \\ \dfrac{\Omega(\mathbf{r}')}{4\pi}, & \mathbf{r}' \in \partial V \\ 1, & \mathbf{r}' \in V \end{cases} \quad (8)$$

where $\Omega(\mathbf{r}')$ is the solid angle lying inside V for the observation point $\mathbf{r}'$.

Boundary Element Method

The concept of BEM is to approximate the surface integral by a sum of discrete boundary elements. For these elements, smaller integrals are solved for a set of observation points, the collocation points. The simplest evaluation method assumes a constant sound pressure on each element and solves for the observed sound pressure by numerical integration, cf. [12]. This yields a linear system of equations which can be written in matrix form

$$\mathbf{Cp} = \mathbf{Hp} - \mathbf{Gp}_n + \mathbf{p}^{\mathbf{I}}, \quad (9)$$

where $\mathbf{C}$ is the $\mathrm{N} \times \mathrm{N}$ diagonal matrix containing the solid angles, $\mathbf{p}$, $\mathbf{p}_n$, and $\mathbf{p}^{\mathbf{I}}$ are $\mathrm{N} \times 1$ vectors containing the total sound pressure, its normal derivative, and the free field sound pressure, respectively, at the N collocation points. $\mathbf{H}$ is the "dipole matrix" and $\mathbf{G}$ the "monopole matrix", each $\mathrm{N} \times \mathrm{N}$ and containing the results of the respective numerical integrals.

For a rigid scatterer, the normal derivatives vanish for collocation points located on its surface, and in this caste (9) reduces to $\mathbf{Cp} = \mathbf{Hp} + \mathbf{p}^{\mathbf{I}}$. Hence, the sound pressure on the surface of a rigid scatterer is yields

$$\mathbf{p} = (\mathbf{H} - \mathbf{C})^{-1}\mathbf{p}^{\mathbf{I}}. \quad (10)$$

All BEM calculations are carried out using *OpenBEM*, a freely available Matlab based toolbox from Peter Moller Juhl and Vicente Cutanda Henriquez [13]. Fig. 3 shows the geometric mesh models used for the BEM calculations.

ANALYSIS OF SPATIAL RESOLUTION

The equations presented before are used to calculate the sound pressure distribution that is considered for the array design in response to any plane wave. In order to evaluate the horizontal and vertical resolution as illustrated in Fig. 4, a set of 2 plane waves are assumed to form the matrix of quasi continuous sound pressure samples $\mathbf{P}^{\mathbf{I}} = [\mathbf{p}^{\mathbf{I}}(\phi_1, \vartheta_1), \mathbf{p}^{\mathbf{I}}(\phi_2, \vartheta_2)]$. For solutions obtained with BEM, the corresponding surface sound pressure is calculated according to the above equation.

$$\mathbf{P} = (\mathbf{H} - \mathbf{C})^{-1}\mathbf{P}^{\mathbf{I}}. \quad (11)$$

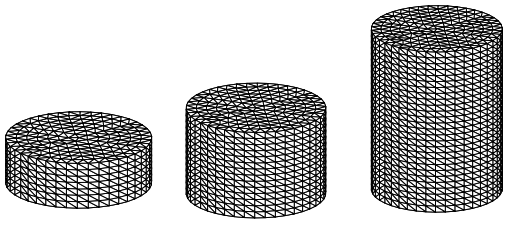

(a) R=1, L=0.5 (b) R=1, L=1 (c) R=1, L=2

Fig. 3. Cylinders models for BEM at different ratios (2:1, 1:1, 1:2) between height and diameter.

One of our particular interests is to find out how the resolution changes with the zenith angle if a cylindrical array is used, in comparison with a spherical array that offers a uniform resolution. Let's assume a set of two plane waves from $\varphi = 0$, centered around the zenith angle ϑ_0 and separated by a space of $\Delta\vartheta$, i.e. $\mathbf{P}^{\mathbf{I}} = [\mathbf{p}^{\mathbf{I}}(\vartheta_0 - \Delta\vartheta/2), \mathbf{p}^{\mathbf{I}}(\vartheta_0 + \Delta\vartheta/2)]$; another pair of plane waves that is 90° rotated with respect to ϑ_0 is used to determine the "horizontal" resolution.

The correlation of the two plane waves with regard to their surface sound pressure $\mathbf{P}$ obtained by Eq. (11) gives us a 2×2 matrix

$$\mathbf{R}(\vartheta_0, \Delta\vartheta) = \mathbf{P}^{\mathrm{H}}\mathbf{P} = \begin{pmatrix} \mathbf{p}_1^{\mathrm{H}}\mathbf{p}_1 & \mathbf{p}_1^{\mathrm{H}}\mathbf{p}_2 \\ \mathbf{p}_2^{\mathrm{H}}\mathbf{p}_1 & \mathbf{p}_2^{\mathrm{H}}\mathbf{p}_2 \end{pmatrix} = \begin{pmatrix} r_{11} & r_{12} \\ r_{12}^{*} & r_{22} \end{pmatrix}. \quad (12)$$

In order to distinguish between these two plane waves, the determinant

$$|\mathbf{R}(\vartheta_0, \Delta\vartheta)| = r_{11}r_{22} - r_{12}^{*}r_{12} \quad (13)$$

must be big enough, i.e. $\sqrt{|\mathbf{R}(\vartheta_0, \Delta\vartheta)|} \geq \mathrm{R}_{\mathrm{th}}$. Herein, R_{th} is a threshold proportional to the squared sound pressure. This measure can be seen to reflect the acoustic properties of a certain geometry concerning the discrimination capabilities of different sound pressure distributions due to different incidence directions.

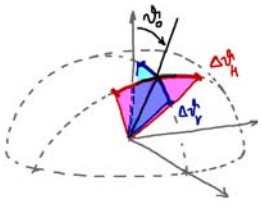

Fig. 4. Geometry of a "vertical" and "horizontal" resolution angle with regard to a reference zenith angle ϑ_0.

RESULTS

The three different configurations shown in Fig. 1 (ring, ribbon, whole surface array) are simulated assuming a dense enough sampling, i.e. the absence of spatial aliasing. For the ribbon-shaped array surface, a fixed height of $\pm 0.5R$ is used. Fig. 5-7 show the spatial resolution that was calculated using Eqs. 12 and 13 choosing a threshold of $R_{th} \geq 0.5$ and two different wavenumbers $k = 0.4$ and $k = 6$. All diagrams are divided into a left half depicting the "vertical" resolution and a right half depicting the "horizontal" resolution.

Fig. 5 shows that ring arrays on the different scatterers cannot resolve waves that are symmetric around the equatorial plane $\vartheta_0 = \pi/2$. This accounts for the typical half space confusion of symmetrical planar arrays. The resolution improves for directions closer to the zenith and nadir, where it is similar to the approximately constant horizontal resolution. Naturally, the resolution is better for the higher wavenumber where one or more wavelengths are sampled by the array. Overall, the resolution of all cylindrical scatterers is similar to the one of the sphere, except for ϑ_0 around zenith or nadir, where it is slightly smaller.

Fig. 6 plots the resolution of ribbon-shaped arrays on the different scatterers. The best horizontal and vertical resolution is similar, and the resolution around the equatorial plane $\vartheta_0 = \pi/2$ strongly improves as the array extends in three dimensional. Again, cylindrical scatterers seem slightly inferior to a spherical one.

Fig. 7 shows the spatial resolution for an active array aperture covering the entire surface of the scatterer. As expected, the full-sampled sphere yields constant resolution in all directions, whereas it is only constant horizontally for the cylinders. The vertical resolution of long cylindrical scatterers with an array spread on the entire surface is naturally better around $\vartheta_0 = \pi/2$ than for a sphere of the same radius.

CONCLUSIONS

We proposed a horizontal and vertical resolution measure to evaluate ring and ribbon-shaped array apertures on cylindrical scatterers. The observation was mostly based on numerical simulations, and analytic formulations were included for the cases of a rigid sphere and the infinite cylinder.

Concluding, the horizontal resolution does not vary much for arrays on different scatterers, even at different zenith angles ϑ_0. It seems that the vertical resolution is merely affected around $\vartheta = \pi/2$ and the difference is deteremined by the height of the effective array aperture. Hence, only the cylinder that is twice as high as wide clearly outperforms a sphercical array in its vertical resolution around the horizontal plane.

Exploiting the scattering off a cylinder to build microphone arrays does not seem to yield a substantially different spatial resolution compared to the sphere and therefore should be further investigated. In our future work, we intend to investigate if cylindrical surface modes can be found that are similarly useful as the spherical harmonics are for spherical arrays.

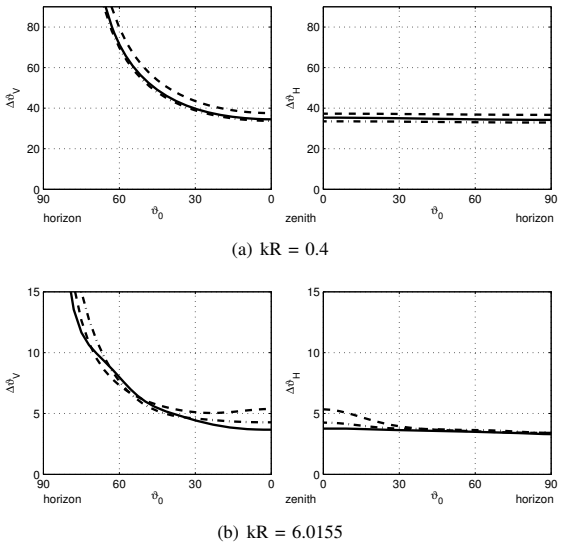

Fig. 5. : Spatial resolution for a ring array on different bodies, cf. Fig. 1. The solid line represents a sphere, the dashed line a cylinder with $R = 1, L = 0.5$ and the dash-dotted line a cylinder with $R = 1, L = 2$.

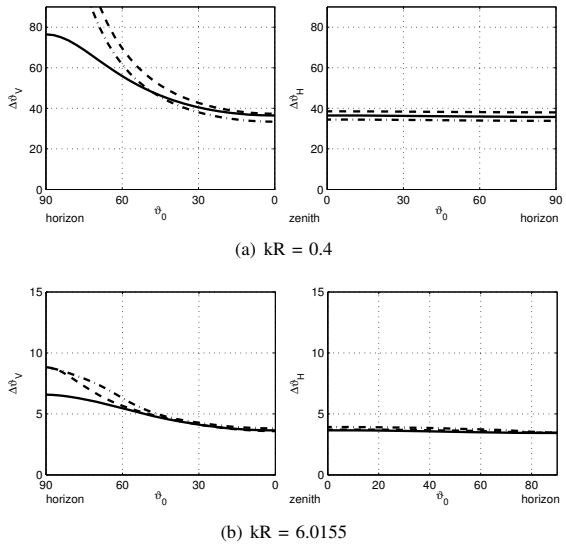

Fig. 6. Spatial resolution for a ribbon array on different bodies, cf. Fig. 1. The solid line represents a sphere, the dashed line a cylinder with $R = 1, L = 0.5$ and the dash-dotted line a cylinder with $R = 1, L = 2$.

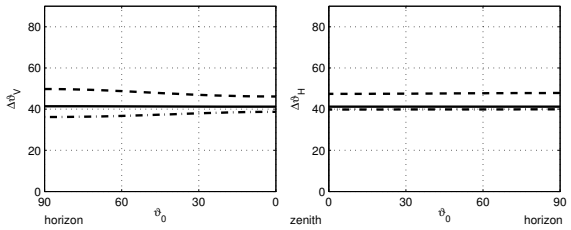

(a) kR = 0.4

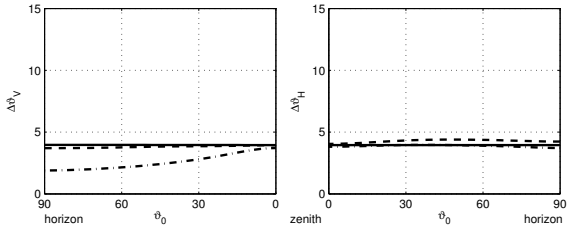

(b) kR = 6.0155

Fig. 7. Spatial resolution for an array fully sampling different bodies, cf. Fig. 1. The solid line represents a sphere, the dashed line a cylinder with $R = 1, L = 0.5$ and the dash-dotted line a cylinder with $R = 1, L = 2$.

REFERENCES

[1] J. Meyer and G. Elko, "A highly scalable spherical microphone array based on an orthonormal decomposition of the soundfield," in Acoustics, Speech, and Signal Processing (ICASSP), 2002 IEEE International Conference on, vol. 2, 2002, pp. II–1781 –II–1784.

[2] T. D. Abhayapala and D. B. Ward, "Theory and design of high order sound field microphones using spherical microphone array," in Acoustics, Speech, and Signal Processing (ICASSP), 2002 IEEE International Conference on, vol. 2, 2002, pp. II–1949 –II–1952.

[3] B. Rafaely, "Analysis and design of spherical microphone arrays," Speech and Audio Processing, IEEE Transactions on, vol. 13, no. 1, pp. 135 – 143, 2005.

[4] Z. Li and R. Duraiswami, "Hemispherical microphone array for sound capture and beamforming," in IEEE Workshop on Applications of Signal Processing to Audio and Acoustics, 2005, 2005.

[5] D. Zotkin, R. Duraiswami, and N. Gumerov, "Plane-wave decomposition of acoustical scenes via spherical and cylindrical microphone arrays," Audio, Speech, and Language Processing, IEEE Transactions on, vol. 18, no. 1, pp. 2 –16, 2010.

[6] H. Teutsch and W. Kellermann, "Acoustic source detection and localization based on wavefield decomposition using circular microphone arrays," The Journal of the Acoustical Society of America, vol. 120, no. 5, pp. 2724–2736, 2006.

[7] H. Teutsch, Modal Array Signal Processing: Principles and Applications of Acoustic Wavefield Decomposition (Lecture Notes in Control and Information Sciences). Secaucus, NJ, USA: Springer-Verlag New York, Inc., 2007.

[8] P. Morse and K. Ingard, Theoretical acoustics. Princeton University Press, 1986.

[9] E. Williams, Fourier acoustics: sound radiation and nearfield acoustical holography. Academic Press, 1999.

[10] R. Ciskowski and C. Brebbia, Boundary element methods in acoustics. Computational Mechanics Publications, 1991.

[11] T. Wu, Boundary element acoustics: fundamentals and computer codes. WIT, 2000.

[12] P.M. Juhl, The boundary element method for sound field calculations. Ph.D. dissertation, Technical University Denmark, 1993.

[13] V. Cutanda Henriquez and P.M. Juhl, OpenBEM – an open source boundary element method software in acoustics. Internoise, 2010.